Climate
of the Past

Open Access

EGU

Supplement of

Antarctic tipping points triggered by the mid-Pliocene warm climate

Javier Blasco et al.

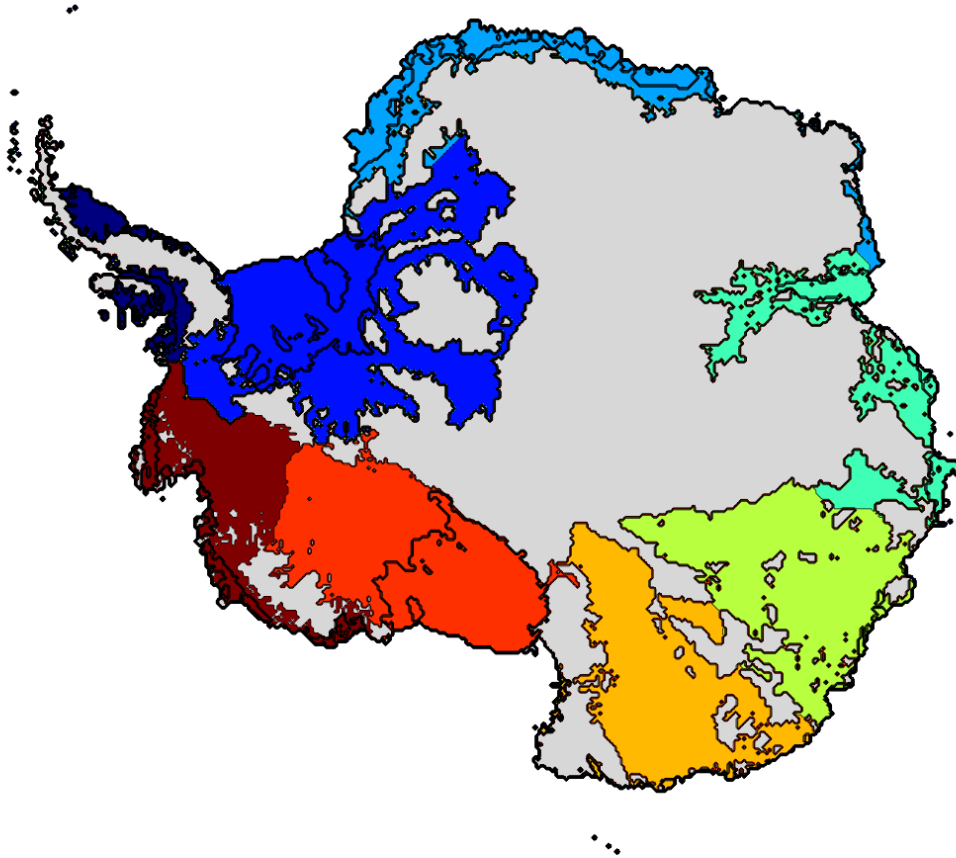*Correspondence to:* Javier Blasco (javier.blasco.navarro@ulb.be)

Figure S1. Map of the Bedrock AIS regions. Navy blue: Antarctic Peninsula. Dark-blue: Filchner-Ronne. Light-blue: North-EAIS. Turkish: Amery. Green: Totten. Orange: Wilkes. Red: Ross. Dark-Red: Amundsen. Gray colors represent bedrock regions above sea level.
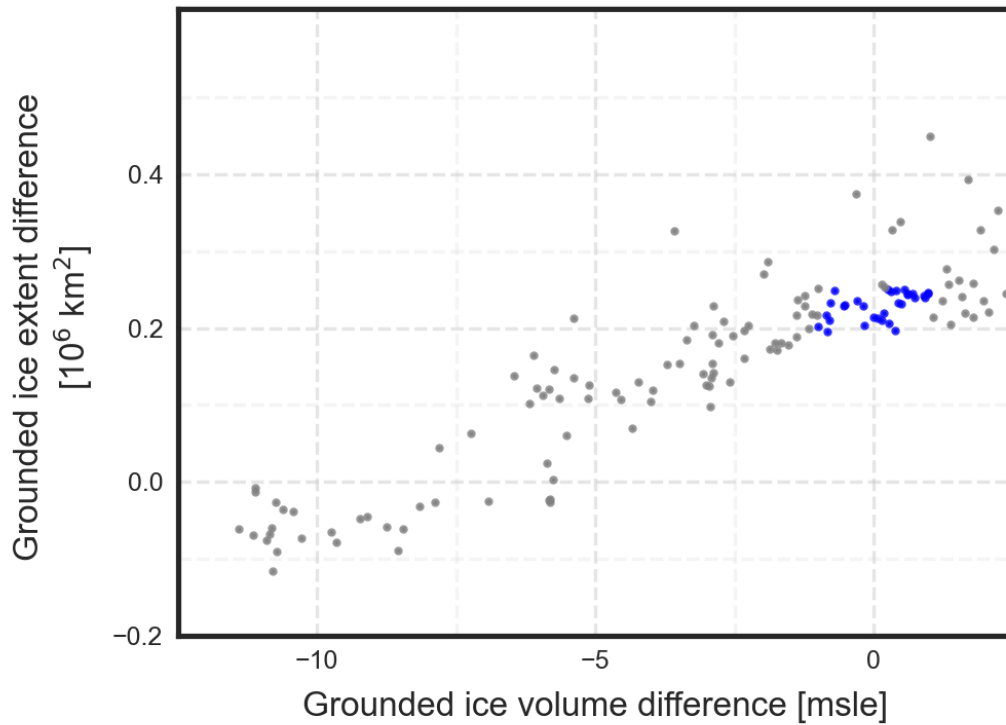
Figure S2. Scatter plot of the Antarctic PD simulations. x-axis represents the grounded ice volume difference between the simulated state and the observations. y-axis represents the grounded ice extent difference between the simulation and the observations. Blue points represent simulations that differ less than 2% from observed values (ice volume and extension) for the AIS and WAIS.
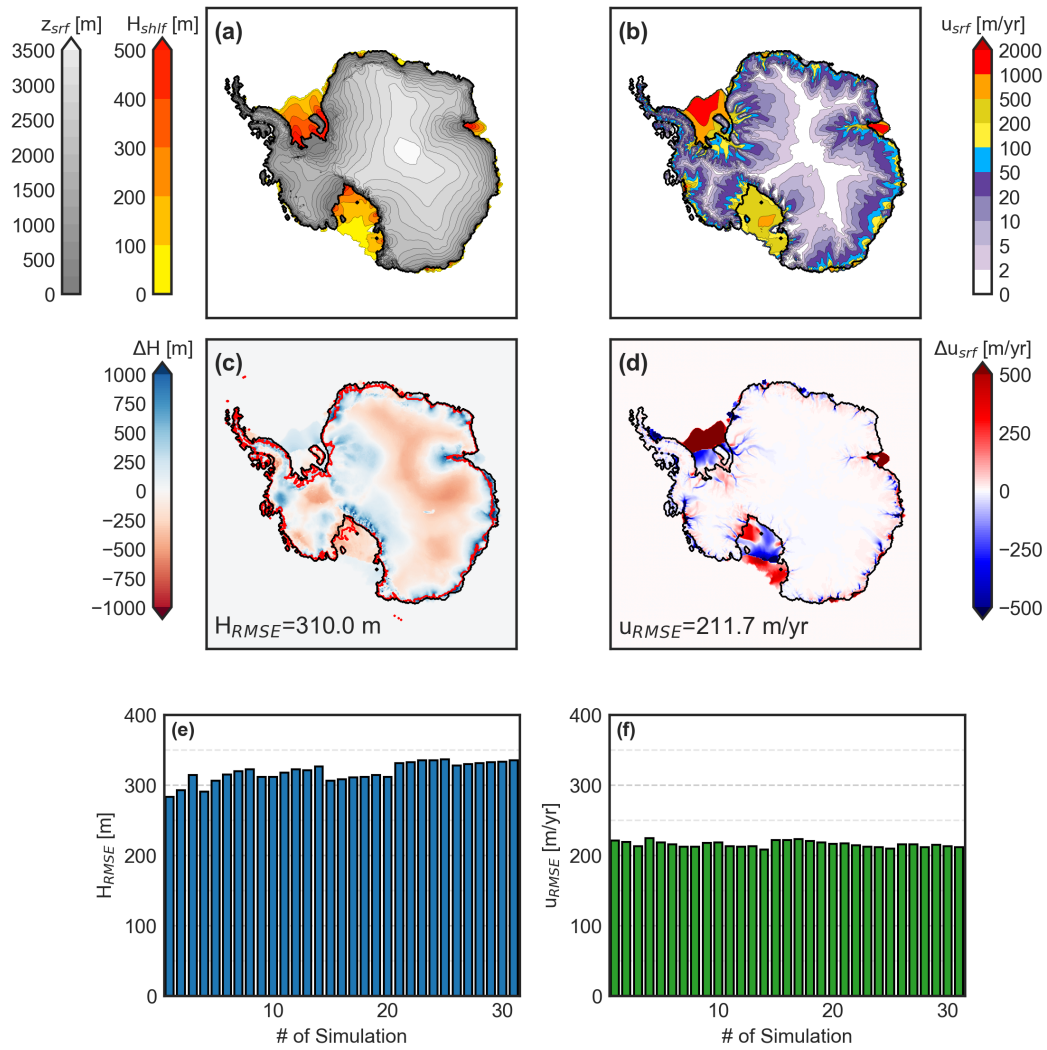
Figure S3. Mean PD state of all the PD simulations. (a) surface elevation (grey colors) and ice shelf thickness (orange); (b) surface velocity; (c) ice thickness (d) surface velocity anomalies with PD observations and its respective RMSE. Bar chart of the simulated PD RMSE in (e) ice thickness and (f) surface velocity for every simulation.
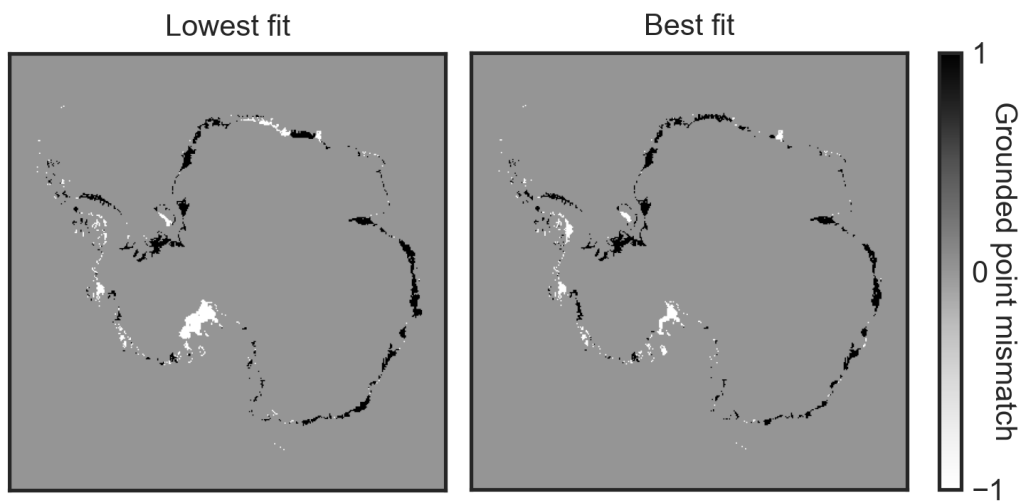
Figure S4. Lowest and best fit of our chosen ensemble parameters. Value zero represents the same mask value between the simulated and the observed ice mask. 1/-1 represent advanced/retreated grounded points with respect to the observations.
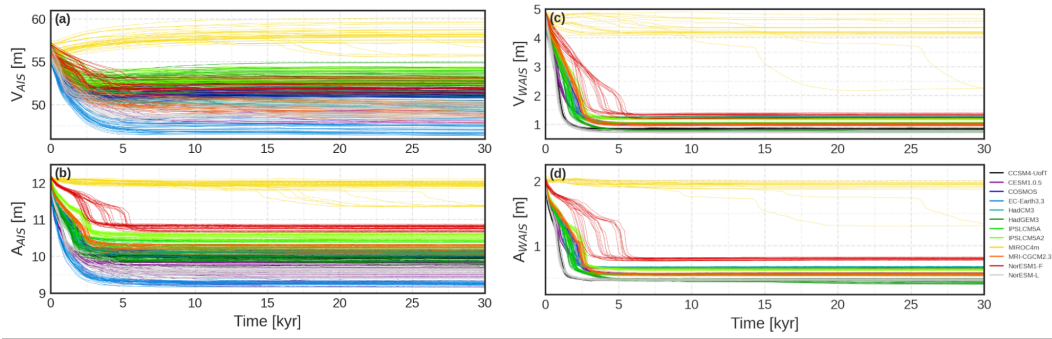
Figure S5. Time evolution of the (a)/(c) AIS/WAIS sea-level content; (b)/(d) AIS/WAIS grounded ice area for the whole ensemble.
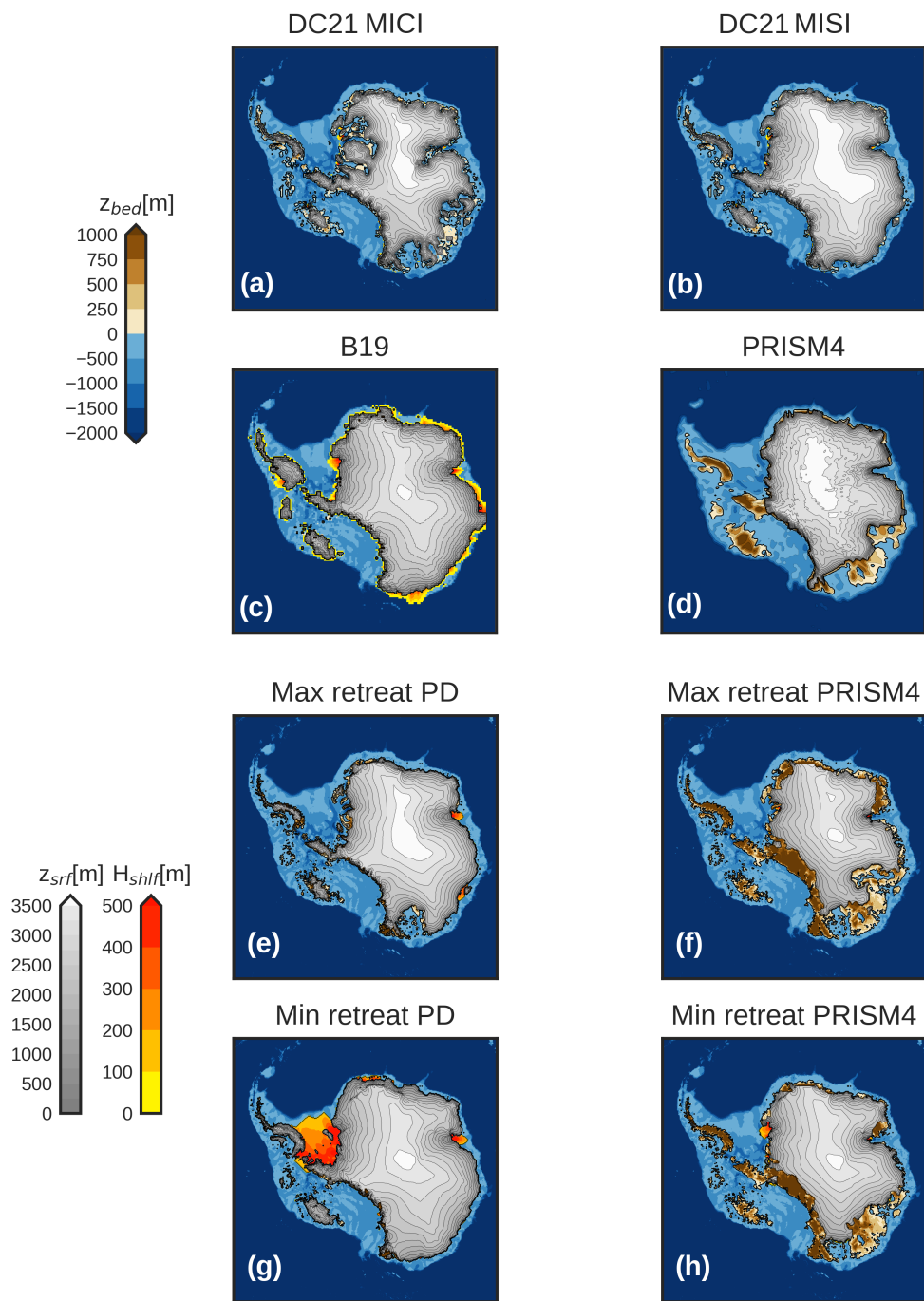
Figure S6. AIS reconstruction/simulations from other studies with surface elevation (gray), floating ice thickness (orange) and bedrock elevation for ice-free points (brown/blue). DeConto et al. (2021) with (a) and without (b) MICI mechanism. (c) Berends et al., (2019) and the (d) PRISM4 boundary conditions for PlioMIP2 (Dowsett et al., 2016). (e)/(f) maximum retreated AIS in our study starting from PD/PRISM4 conditions. (g)/(h) minimum retreated AIS in our study starting from PD/PRISM4 conditions.

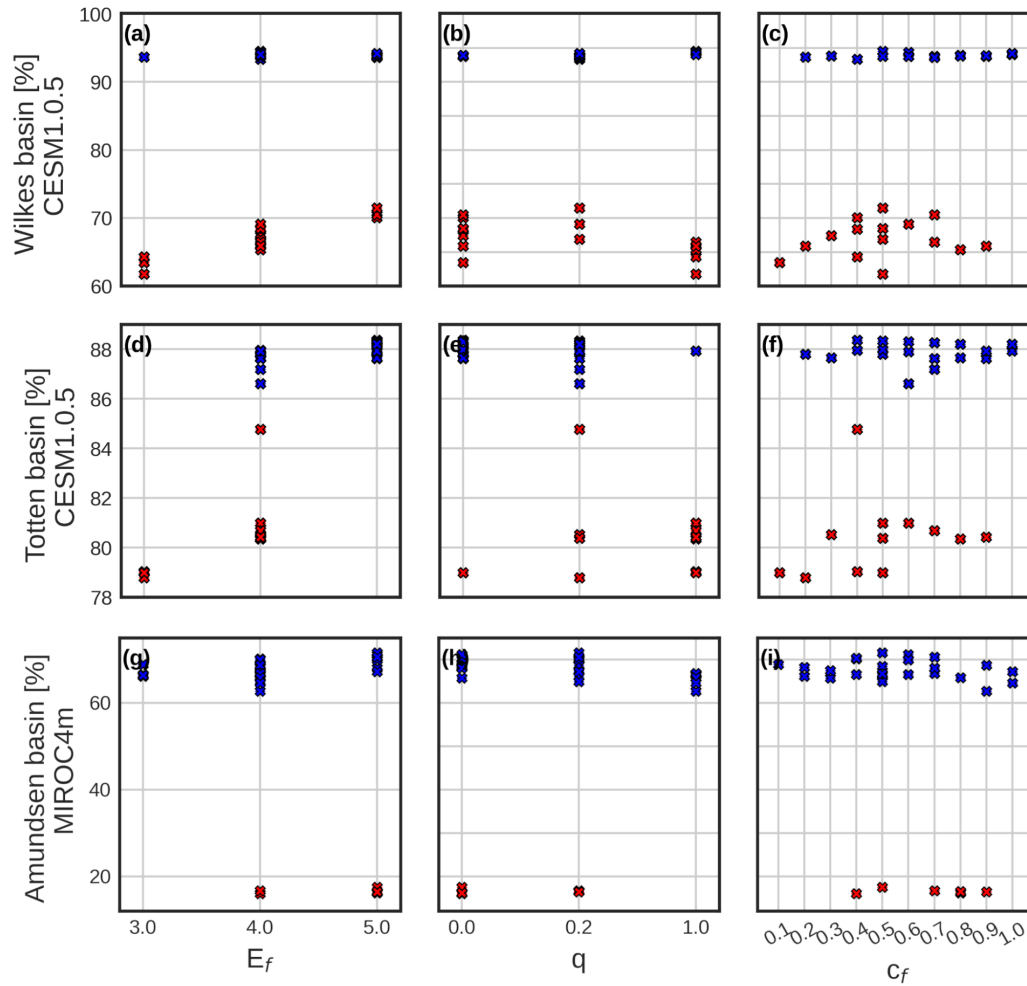**Figure S7.** Scatter plot of (a)/(d)/(g) enhancement factor; (b)/(e)/(h) Friction law exponent; (c)/(f)/(i) friction coefficient with respect to the Wilkes, Totten and Amundsen basin ice area. Top/Center and Lower row shows the CESM1.0.5/MIROC4m models. Red/Blue colors represent collapsed/non-collapsed states.

AOGCM	CMIP6	Ocean	AIS contribution to sea-level rise$_{Q_1}^{Q_3}$ (m)	Reference
CCSM4-UofT	No	No	$4.7_{-0.1}^{+0.3}$	Chandan and Peltier (2017)
CESM1.0.5	No	Yes	$6.0_{-1.3}^{+1.8}$	Baatsen et al. (2022)
COSMOS	No	Yes	$4.6_{-0.1}^{+0.2}$	Stepanek et al. (2020)
EC-Earth3.3	Yes	Yes	$8.9_{-0.3}^{+0.2}$	Zhang et al. (2021)
HadCM3	No	Yes	$5.9_{-0.2}^{+0.1}$	Hunter et al. (2019)
HadGEM3	Yes	Yes	$2.7_{-0.4}^{+0.1}$	Williams et al. (2021)
IPSLCM5A	No	No	$3.4_{-0.3}^{+0.4}$	Tan et al. (2020)
IPSLCM5A2	No	No	$2.9_{-0.1}^{+0.1}$	Tan et al. (2020)
MIROC4m	No	Yes	$-1.9_{-0.4}^{+0.3}$	Chan and Abe-Ouchi (2020)
MRI-CGCM2.3	No	No	$7.0_{-0.1}^{+0.3}$	Kamae et al. (2016)
NorESM1-F	No	Yes	$4.0_{-0.1}^{+0.3}$	Li et al. (2020)
NorESM-L	No	Yes	$6.8_{-0.1}^{+0.1}$	Li et al. (2020)

Table S1. Table summarizing the AOGCMs, its contributon to CMIP6, if ocean files are available and the contribution in this study to sea-level rise and its range between the 3rd and 1st quartile.

References

Baatsen, M. L., von der Heydt, A. S., Kliphuis, M. A., Oldeman, A. M., and Weiffenbach, J. E.: Warm mid-Pliocene conditions without high climate sensitivity: the CCSM4-Utrecht (CESM 1.0. 5) contribution to the PlioMIP2, Climate of the Past, 18, 657–679, https://doi.org/10.5194/cp-18-657-2022, 2022.

5 Chan, W.-L. and Abe-Ouchi, A.: Pliocene Model Intercomparison Project (PlioMIP2) simulations using the Model for Interdisciplinary Research on Climate (MIROC4m), Climate of the Past, 16, 1523–1545, https://doi.org/10.5194/cp-16-1523-2020, 2020.

Chandan, D. and Peltier, W. R.: Regional and global climate for the mid-Pliocene using the University of Toronto version of CCSM4 and PlioMIP2 boundary conditions, Climate of the Past, 13, 919–942, https://doi.org/10.5194/cp-13-919-2017, 2017.

Hunter, S. J., Haywood, A. M., Dolan, A. M., and Tindall, J. C.: The HadCM3 contribution to PlioMIP phase 2, Climate of the Past, 15,
10 1691–1713, https://doi.org/10.5194/cp-15-1691-2019, 2019.

Kamae, Y., Yoshida, K., and Ueda, H.: Sensitivity of Pliocene climate simulations in MRI-CGCM2. 3 to respective boundary conditions, Climate of the Past, 12, 1619–1634, https://doi.org/10.5194/cp-12-1619-2016, 2016.

Li, X., Guo, C., Zhang, Z., Otterå, O. H., and Zhang, R.: PlioMIP2 simulations with NorESM-L and NorESM1-F, Climate of the Past, 16, 183–197, https://doi.org/10.5194/cp-16-183-2020, 2020.

15 Stepanek, C., Samakinwa, E., Knorr, G., and Lohmann, G.: Contribution of the coupled atmosphere–ocean–sea ice–vegetation model COSMOS to the PlioMIP2, Climate of the Past, 16, 2275–2323, https://doi.org/10.5194/cp-16-2275-2020, 2020.

Tan, N., Contoux, C., Ramstein, G., Sun, Y., Dumas, C., Sepulchre, P., and Guo, Z.: Modeling a modern-like p CO 2 warm period (Marine Isotope Stage KM5c) with two versions of an Institut Pierre Simon Laplace atmosphere–ocean coupled general circulation model, Climate of the Past, 16, 1–16, https://doi.org/10.5194/cp-16-1-2020, 2020.

20 Williams, C. J., Sellar, A. A., Ren, X., Haywood, A. M., Hopcroft, P., Hunter, S. J., Roberts, W. H., Smith, R. S., Stone, E. J., Tindall, J. C., et al.: Simulation of the mid-Pliocene Warm Period using HadGEM3: experimental design and results from model–model and model–data comparison, Climate of the Past, 17, 2139–2163, https://doi.org/10.5194/cp-17-2139-2021, 2021.

Zhang, Q., Berntell, E., Axelsson, J., Chen, J., Han, Z., De Nooijer, W., Lu, Z., Li, Q., Zhang, Q., Wyser, K., et al.: Simulating the mid-Holocene, last interglacial and mid-Pliocene climate with EC-Earth3-LR, Geoscientific Model Development, 14, 1147–1169,
25 https://doi.org/10.5194/gmd-14-1147-2021, 2021.